DOI: 10.61782/fa.2025.0133

FORUM ACUSTICUM
EURONOISE 2025

ANALYSIS OF THE RELATIONSHIP BETWEEN SOUND FIELD ISOTROPY AND ERRORS IN THE RESULTS OF SABINE'S ABSORPTION COEFFICIENT.

Marco Berzborn and Michael Vorländer
Institute for Hearing Technology and Acoustics, RWTH Aachen University, Germany

ABSTRACT

Sabine's absorption coefficient is measured in a reverberation rooms under the assumption of a diffuse sound field. Recently multiple authors presented experimentally approaches using microphone arrays to quantify sound field diffuseness within the context of absorption measurements, indeed highlighting the lack of a diffuse sound field for specific lab environments and frequency bands. This was found to be especially prominent when the absorbing test specimen is mounted in the room.
This work presents a combined factor analysis and linear regression model to investigate the relationship between the results of the aforementioned diffuseness quantification methods and the error in Sabine's absorption coefficient. A numerically predicted finite size absorption coefficient serves as ground truth to calculate the relative error in the absorption coefficient. Finally, the suitability of the model to correct the measurements of Sabine's absorption coefficient is analyzed.

Keywords: reverberation, directional energy decay, microphone array

1. INTRODUCTION

The measurement of Sabine's absorption coefficient according to ISO354:2003 [1] is performed in a reverberation room under the assumption of a diffuse sound field. While the method is widely used since the 1920s, it is well known to suffer from a poor reproducibility between laboratories. This has been shown in several inter-laboratory studies, see for example Refs. [2] and [3]. See Ref. [4] for a overview of the issues associated with the measurement of Sabine's absorption coefficient. Recent studies studies have indeed shown that the sound field in reverberation rooms is indeed not perfectly diffuse, or more precisely not isotropic [5], [6] This was found to be especially prominent when the absorbing specimen is mounted in the room.
To statistically investigate the relationship between the isotropy condition of the sound field in the laboratory and the error in Sabine's absorption coefficient which is calculated as per ISO354:2003 [1] a regression model is developed in this work. The input and output data-sets, as well as the regression model are derived in Section 2. The experimental setup consisting of three different laboratory conditions is described in Section 3. Section 4 and Section 5 present the implementation of the regression model and the results, respectively, followed by a conclusion in Section 6.

*__Corresponding author__: mbe@akustik.rwth-aachen.de.

2. MODEL

2.1 Target Variables

As target variables for the regression model developed in this section, the relative error in Sabine's absorption coefficients are used. These are computed for the T_{20}, T_{30}, and T_{40} regression intervals

$$\varepsilon_j = \frac{\bar{\alpha}_j - \tilde{\alpha}}{\tilde{\alpha}}, \quad j \in \{20, 30, 40\}, \tag{1}$$

where $\tilde{\alpha}$ is a reference finite-size random-incidence absorption coefficient estimated using a combined finite element and boundary element method simulation similar to Ref. [7]. Material parameters were inferred from

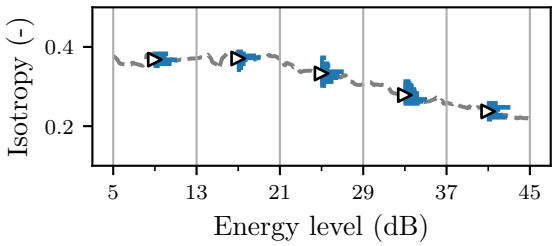

Figure 1: Isotropy evolution (- - -) as function of the decay level as well as the histogram (▬) of the indicated 8 dB intervals and their respective mean (▷).

impedance tube measurements using the method presented in Ref. [8]. Here, the relative error is chosen as it is independent from the absolute magnitude of the absorption coefficient.

2.2 Input Variables

The input data for the model is derived from the temporal evolution of estimators for sound field isotropy and axial symmetry. These estimators are calculated according to Berzborn *et al.* [9]. The isotropy estimator is based on Ref. [5] and the axial symmetry estimator is inspired by the work of Jammalamadaka and Terdik [10]. Both quantifiers are linearly interpolated to a common scale proportional to the decay level of the respective omnidirectional Energy Decay Curve (EDC). This normalization also aligns the evolution of the quantifiers with the reverberation time evaluation ranges. In addition to the estimator magnitude, their rate of change is of interest as well. This information is captured in the first derivative of the quantifiers with respect to the energy level.

The quantifiers are averaged over decay level intervals of 8 dB. The interval is chosen small enough such that the distributions of the data within the interval is uni-modal and is well represented by its mean. In agreement with ISO354:2003 [1], the initial 5 dB of the decay process are excluded from the analysis. The lowest energy level used is -45 dB due to the limited dynamic range of the Directional Energy Decay Curve (DEDC) measurements. An example of the process for the isotropy evolution is given in Fig. 1. Derivatives are typically sufficiently represented by averaging over the entire decay process.

This results in 12 input variables for each frequency band and room configuration. In the following, a matrix $\mathbf{\Gamma} \in \mathbb{R}^{12\times O}$ is constructed by stacking the vectors $\boldsymbol{\gamma}$ for all rooms and frequency bands. To ensure equal weighting of the symmetry quantifiers and their derivatives, the data are normalized to zero mean and unit variance Yong and Pearce [11].

2.3 Factor Analysis Regression

Since the symmetry quantifiers are derived from the same underlying data, they are expected to be correlated. The correlation is expected to be even stronger for cases where consecutive segmentation intervals show similar mean values, as is the case for configurations and frequency bands with uniform damping distribution. In order to identify a set of underlying latent variables and at the same time reduce the dimensionality of the input data vector a factor analysis is performed. The factor analysis is designed to explain the matrix of observations by a linear combination of the latent variables. In matrix notation, the factor analysis model can be written as [11]

$$\mathbf{\Gamma} = \mathbf{\Psi}\mathbf{Z} + \mathbf{N}, \tag{2}$$

where $\mathbf{\Psi} \in \mathbb{R}^{12\times Z}$ is the factor loading matrix, $\mathbf{Z} \in \mathbb{R}^{Z\times O}$ is the matrix of latent variables, and $\mathbf{N} \in \mathbb{R}^{12\times O}$ is an additive residual error matrix. The factor loading matrix is estimated iteratively from the correlation matrix of the input data using orthogonal *quartimax* rotations.

Assuming a linear relationship between the latent variables and the absorption coefficient error, a multiple linear regression model is used, which is expressed as

$$\boldsymbol{\varepsilon} = \boldsymbol{\beta}\hat{\mathbf{Z}} + \mathbf{n}_\varepsilon, \tag{3}$$

where $\boldsymbol{\varepsilon} \in \mathbb{R}^{3\times O}$ is the matrix containing the stacked vectors of absorption coefficient errors calculated for the three reverberation time intervals, $\boldsymbol{\beta} \in \mathbb{R}^{Z}$ is the vector of regression coefficients

$$\boldsymbol{\beta} = [\beta_0, \beta_1, \ldots, \beta_Z]^\mathsf{T}, \tag{4}$$

where β_0 is the intercept and $\mathbf{n}_\varepsilon \in \mathbb{R}^{O}$ represents the additive modeling error. The matrix $\hat{\mathbf{Z}}$ is obtained by adding a column of ones to the matrix of latent variables $\mathbf{Z}$ to account for the intercept term.

2.4 Absorption Coefficient Prediction

Once the factor loading matrix and the regression coefficients are identified, the model can re-arranged to predict a corrected version of Sabine's absorption coefficient based on the symmetry quantifiers. Replacing the reference absorption coefficient $\tilde{\alpha}$ in Eq. (1) with the predicted

absorption coefficient $\hat{\alpha}_j$, the corrected absorption coefficient can be computed as

$$\hat{\alpha}_j = \bar{\alpha}_j(1+\varepsilon_j) \quad j \in \{20, 30, 40\}. \tag{5}$$

Substituting Eq. (3) into Eq. (5) results in

$$\hat{\boldsymbol{\alpha}} = \bar{\boldsymbol{\alpha}} \odot \left(1 + \boldsymbol{\beta}\hat{\mathbf{Z}}\right), \tag{6}$$

where $\hat{\boldsymbol{\alpha}} \in \mathbb{R}^{3\times O}$ and $\bar{\boldsymbol{\alpha}} \in \mathbb{R}^{3\times O}$ are the matrices containing the corrected and measured absorption coefficients, respectively, and $\odot$ denotes the Hadamard product.

3. EXPERIMENTAL SETUP

The spherical and axial symmetry quantifiers were computed from experimental data captured in three different laboratory conditions: A rectangular reverberation room with volume $245\,\mathrm{m}^3$ in a configuration including 22 panel diffusers and a second configuration without any diffuser treatment – referred to as room no. 1 – and a second reverberation room with volume $215\,\mathrm{m}^3$ equipped with a combination of 12 panel and 85 boundary diffusers – referred to as room no. 2. The same glass-wool test specimen with $10.8\,\mathrm{m}^2$ was used in all laboratory conditions.

A Universal Robots UR5 scanning robotic arm was used to sequentially sample a dual-radius spherical microphone array. The sequential microphone array consists of a total of 310 sampling positions including interior points to stabilize the eigenfrequencies of the sphere. Their positions were calculated using the algorithm proposed by Chardon *et al.* [12]. Three different receiver positions were used in room no. 1, while only two receiver positions were used in room no. 2. For each condition, a single source position was used. The procedure to calculate the symmetry quantifiers is outlined in Ref. [9].

The reverberation time used to estimate the respective absorption coefficients was calculated from the omnidirectional EDC at the center position of the microphone array. Instead of using an additional measurement, the omnidirectional EDC was computed as the Schroeder [13] integral of the monopole moment of the omnidirectional response of the microphone array.

Note that while the setup is as similar to the procedure described in ISO354:2003 [1] as possible, it does not fully comply with the standard in the following aspects:

- The number of source and receiver positions per laboratory condition is far lower than the minimum number of 12 required by the standard.
- No frame was used to cover the specimen's sides, which is accounted for in the numerically calculated reference absorption coefficient.

4. MODEL IMPLEMENTATION

The factor analysis and multiple linear regression model were implemented based on the *scikit-learn* library, [14]. In order to later validate the model, a split of the data into a training and test set was performed, where the training set consisted of 75 % of the full dataset. The suitability of the input data for factor analysis was assessed using the Bartlett [15] test of sphericity and the Kaiser-Meyer-Olkin measure of sampling adequacy [11]. The number of latent variables used in the factor analysis was determined using a *scree* plot, and consecutively confirmed using a parallel analysis as suggested by Horn [16]. Estimation of the loading matrix was performed iteratively using the maximum likelihood approach. The linear regression based on the latent variables was performed using a standard least squares approach. A significance test of the regression coefficients was performed using an Analysis of Variances (ANOVA) on the regression models for the three reverberation time intervals. Additional significance tests of the individual regression coefficients were performed using *t*-tests.

5. RESULTS

The results presented in this chapter are based on the symmetry estimator input data derived for the occupied rooms. If not otherwise stated the presented results are based on the training data set.

5.1 Factor Analysis

The factor analysis indicated that the input data can be represented by three latent variables. Most prominently, the first latent variable represents the quantitative value of the isotropy and axial symmetry estimators, with high loadings for all respective intervals. Similarly, the second latent variable primarily represents the rate of change of the symmetry quantifiers. Interestingly, increased loading is also observed for the input variables representing the quantity of both estimators towards the late part of the decay process. This is most likely due to the fact that this part of the decay process shows the largest rate of change in the symmetry quantifiers in the case of non-uniform damping, see for example. Fig. 1. Such cross-loading of

input-variables on multiple latent factors indicates non-ideal separation of the latent variables. Nonetheless, the second latent variable may still be interpreted as the rate of change of the symmetry quantifiers.
In comparison, the third latent variable shows overall lower and slightly inconsistent loadings for all variables, and as a result is not clearly interpretable. As the next section will show, the third latent variable does not contribute significantly to the developed model.

5.2 Multiple Linear Regression

The ANOVA results indicate that the regression model is significant at a level $p < 0.001$ for all reverberation time intervals, with F-statistics of 44.9, 80.7, and 88.4, see Table 1. The individual t-tests of the regression coefficients indicate that all except β_3 are statistically significant with $p < 0.001$. For β_3, that is the third latent variable, the T-statistic is subject to low values while the p-values are between 0.12 and 0.41, indicating that the third latent variable does not significantly contribute to the model. As mentioned before, the third latent variable is consequently excluded from the model for the remaining analysis.

As a goodness of fit measure, the coefficient of determination R^2 was computed. For the training data set the coefficient of determination is found to increase with increasing dynamic range used for calculation of the reverberation time, showing values from 0.75 to 0.86, see Table 1. For the test data the R^2 and mean squared error are found to be slightly lower than for the training data, with R^2 values of 0.68 to 0.80, see Table 1. While the test data shows slightly lower accuracy, the results still indicate sufficient generalization capabilities of the model.

Figure 2 shows the regression lines for the individual latent variables separately, as well as the 95 % confidence interval, and the individually calculated R^2 measure. Each row corresponds to one of the reverberation time intervals. The increase of the reverberation time interval seemingly improves the accuracy of the model. In fact, Fig. 2 reveals that the increase in the goodness of fit is primarily due to the improved goodness of fit for the second latent variable. Interestingly, the R^2 measure obtained for the first latent variable is found to be similar for ε_{20}, ε_{30}, and ε_{40} with values between 0.64 to 0.68, while the R^2 measure for the second latent variable increases from 0.09 to 0.22. This may indicate two things: Firstly, the magnitude of the symmetry estimators is more indicative for the error in the absorption coefficient than their respective rate of change for the given model. Secondly, the rate of change in the symmetry quantifiers reflects the increase in the reverberation time estimation error – and hence increase in the absorption coefficient error – for larger evaluation intervals in the presence of multi-exponential energy decay. Note that the R^2 for the second latent variable is still low for all reverberation time intervals. This is also due to a number of distinct outliers. For the second latent variable outliers for $\Psi_2 > 0$ and $\varepsilon < -0.3$ are observed which result in an increased regression error for all reverberation time intervals, cf. Fig. 2. Similarly, outliers are observed for the first latent variable for $\varepsilon < -0.3$ and $\Psi_1 < 1$, cf. Fig. 2. While the outliers are not clearly interpretable, it is highly likely that they are due to insufficient separation of the input variables, which was already hinted at in the interpretation of the factor analysis.

Table 1: Results of the F-test, as well as the coefficient of determination R^2 for the multiple linear regression model. The F-test statistics are given for the training data only.

			R^2	
	F-statistic	p-value	Training	Test
ε_{20}	44.9	< 0.001	0.75	0.68
ε_{30}	80.7	< 0.001	0.85	0.81
ε_{40}	88.4	< 0.001	0.86	0.80

5.3 Absorption Coefficient Prediction

Figure 3 shows the corrected absorption coefficient (using Eq. (6)) without distinguishing between training and test data, as well as the measured absorption coefficient.Further, Fig. 3 shows the numerically computed finite size absorption coefficient. The depicted data for each frequency band corresponds to the average over three all laboratory rooms and receiver positions. The results indicate that the mean of the corrected absorption coefficient is in good agreement with the reference absorption coefficient for the T_{20}, T_{30}, and T_{40} intervals. Further, the $[2.5\,\%, 97.5\,\%]$ percentiles of the corrected absorption coefficient are smaller compared to the respective percentiles of the measured data. Interestingly, the agreement seems best for the T_{20} interval, and decreases with increasing

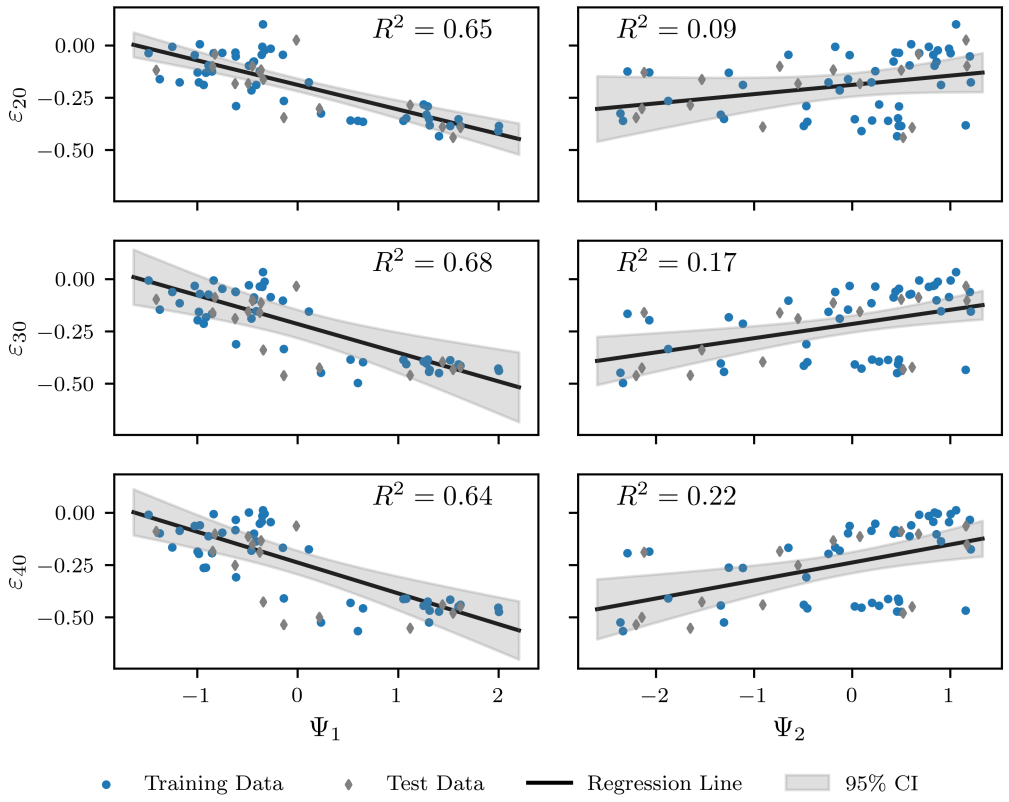

Figure 2: Regression lines for the two predicted relative absorption coefficient error based on the two latent variables. Shaded areas indicate the 95 % confidence interval.

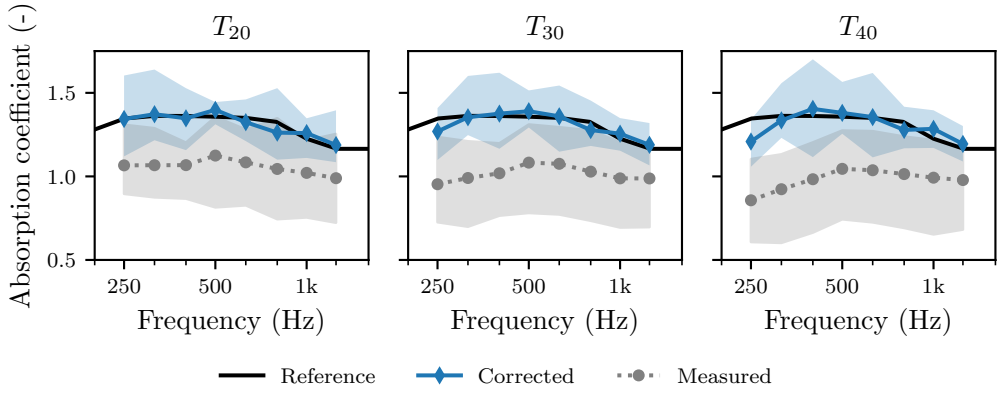

Figure 3: Mean of the corrected and measured absorption coefficient data averaged over all laboratory rooms. Shaded areas indicate the region spanning the 2.5 % and 97.5 % percentiles. The combined test and training data are used. The reference refers to the numerically computed absorption coefficient.

reverberation time evaluation interval which seems counterintuitive as the interval showed the lowest R^2 in the previous section.
An additional room by room analysis revealed that the high variance of the corrected absorption coefficient is primarily influenced by the room configuration without panel diffusers installed for most frequency bands.Similarly, the variance in the measured absorption coefficient is primarily influenced by the room configuration without panel diffusers installed.This observation is in agreement with the results of the previous section, which showed that the outliers in the regression model are primarily associated with the room configuration without panel diffusers installed.

6. CONCLUSION

This paper presented a stochastic model for the analysis between the uniformity of incident energy distributions – i.e. isotropy and axial symmetry – and the error in Sabine's absorption coefficient. The results indicate a statistically significant relationship. While the results of the regression model are promising, the analysis of the relationship between the latent variables and the absorption coefficient error revealed mismatches between the target data and the model. A number of distinct outliers were observed, which are most likely due to insufficient separation of the latent variables in the factor analysis. Future work should involve the development of an improving the identification of the latent variables. Especially a model-based parameterization of the symmetry quantifiers, is expected to improve the performance of the regression model. Nevertheless, initial results indicate that the model can be used to correct Sabine's absorption coefficient if data from multiple laboratory rooms are available to train the model.

7. ACKNOWLEDGMENTS

The authors would like to thank Melanie Nolan and Efren Fernandez Grande for the collaboration on the measurement campaign and Manuj Yadav for the fruitful discussions on the statistic model.
We would like to thank the Deutsche Forschungsgemeinschaft (DFG) for funding parts of this work under grant number 298797807.

8. REFERENCES

[1] ISO354:2003, *ISO 354:2003 - Measurement of sound absorption in a reverberation room*, 2003.

[2] R. E. Halliwell, "Inter-laboratory variability of sound absorption measurement," *J. Acoust. Soc. Am.*, vol. 73, no. 3, pp. 880–886, Mar. 1983. DOI: 10.1121/1.389011.

[3] C. Scrosati, F. Martellotta, F. Pompoli, *et al.*, "Towards more reliable measurements of sound absorption coefficient in reverberation rooms: An Inter-Laboratory Test," *Appl. Acoust.*, vol. 165, p. 107 298, Aug. 2020. DOI: 10.1016/j.apacoust.2020.107298.

[4] J. Balint, M. Berzborn, M. Nolan, and M. Vorländer, "Measuring Sound Absorption: The Hundred-Year Debate on the Reverberation Chamber Method," *Acoust. Today*, vol. 19, no. 3, p. 13, 2023. DOI: 10.1121/AT.2023.19.3.13.

[5] M. Nolan, M. Berzborn, and E. Fernandez-Grande, "Isotropy in decaying reverberant sound fields," *J. Acoust. Soc. Am.*, vol. 148, no. 2, pp. 1077–1088, Aug. 2020. DOI: 10.1121/10.0001769.

[6] M. Berzborn, M. Nolan, E. Fernandez-Grande, and M. Vorländer, "Comparison of Isotropy Estimators for the Analysis of Reverberation Rooms," in *E-Forum Acusticum*, e-Forum Acusticum 2020, 2020, pp. 139–146. DOI: 10/gqj4b9.

[7] M. Pereira, P. Mareze, L. Godinho, P. Amado-Mendes, and J. Ramis, "Proposal of numerical models to predict the diffuse field sound absorption of finite sized porous materials – BEM and FEM approaches," *Appl. Acoust.*, vol. 180, p. 108 092, Sep. 2021. DOI: 10.1016/j.apacoust.2021.108092.

[8] M. Berzborn and M. Vorländer, "Inference of the Acoustic Properties of Transversely Isotropic Porous Materials," in *Proceedings Of Internoise*, Nantes, 2024, pp. 1–6.

[9] M. Berzborn, M. Nolan, E. Fernandez-Grande, and M. Vorländer, "Directional sound field decay analysis in a reverberation room," *J. Acoust. Soc. Am.*, vol. under review, 2024.

[10] S. R. Jammalamadaka and G. H. Terdik, "Harmonic analysis and distribution-free inference for spherical distributions," *J. Multivar. Anal.*, vol. 171, no. 5, pp. 436–451, May 2019. DOI: 10.1016/j.jmva.2019.01.012.

[11] A. G. Yong and S. Pearce, "A Beginner's Guide to Factor Analysis: Focusing on Exploratory Factor Analysis," *TQMP*, vol. 9, no. 2, pp. 79–94, Oct. 12, 2013. DOI: 10.20982/tqmp.09.2.p079.

[12] G. Chardon, W. Kreuzer, and M. Noisternig, "Design of spatial microphone arrays for sound field interpolation," *IEEE J. Sel. Topics Signal Process.*, vol. 9, no. 5, pp. 780–790, 2015. DOI: 10.1109/JSTSP.2015.2412097.

[13] M. R. Schroeder, "New Method of Measuring Reverberation Time," *J. Acoust. Soc. Am.*, vol. 37, no. 6, pp. 1187–1187, 1965. DOI: 10.1121/1.1939454.

[14] F. Pedregosa, G. Varoquaux, A. Gramfort, *et al.*, "Scikit-learn: Machine Learning in Python," *J. Mach. Learn. Res.*, vol. 12, no. 85, pp. 2825–2830, 2011.

[15] M. S. Bartlett, "Properties of Sufficiency and Statistical Tests," *Proceedings of the Royal Society of London. Series A, Mathematical and Physical Sciences*, vol. 160, no. 901, pp. 268–282, 1937. JSTOR: 96803.

[16] J. L. Horn, "A rationale and test for the number of factors in factor analysis," *Psychometrika*, vol. 30, no. 2, pp. 179–185, Jun. 1, 1965. DOI: 10.1007/BF02289447.